ICES Journal of Marine Science Advance Access published March 15, 2011

ICES Journal of Marine Science; doi:10.1093/icesjms/fsr008

Predicting the effects of climate change on bluefin tuna (*Thunnus thynnus*) spawning habitat in the Gulf of Mexico

Barbara A. Muhling[1,2]*, Sang-Ki Lee[1,3], John T. Lamkin[2], and Yanyun Liu[1,3]

[1]*Cooperative Institute for Marine and Atmospheric Studies, University of Miami, Coral Gables, FL 33146, USA*
[2]*Southeast Fisheries Science Center, NOAA National Marine Fisheries Service, 75 Virginia Beach Drive, Miami, FL 33149, USA*
[3]*NOAA Atlantic Oceanographic and Meteorological Laboratory, 4301 Rickenbacker Causeway, Miami, FL 33149, USA*

**Corresponding Author: tel: +1 305 361 4289; fax: +1 305 365 4103; e-mail: barbara.muhling@noaa.gov.*

Muhling, B. A., Lee, S-K., Lamkin, J. T., and Liu, Y. Predicting the effects of climate change on bluefin tuna (*Thunnus thynnus*) spawning habitat in the Gulf of Mexico. – ICES Journal of Marine Science, doi:10.1093/icesjms/fsr008.

Received 1 July 2010; accepted 6 January 2011.

Atlantic bluefin tuna (BFT) is a highly migratory species that feeds in cold waters in the North Atlantic, but migrates to tropical seas to spawn. Global climate-model simulations forced by future greenhouse warming project that upper-ocean temperatures in the main western Atlantic spawning ground, the Gulf of Mexico (GOM), will increase substantially, potentially altering the temporal and spatial extent of BFT spawning activity. In this study, an ensemble of 20 climate model simulations used in the Intergovernmental Panel for Climate Change fourth Assessment Report (IPCC-AR4) predicted mean temperature changes within the GOM under scenario A1B through to 2100. Associations between adult and larval BFT in the GOM and sea temperatures were defined using 20th century observations, and potential effects of warming on the suitability of the GOM as a spawning ground were quantified. Areas in the GOM with high probabilities of larval occurrence decreased in late spring by 39–61% by 2050 and 93–96% by the end of the 21st century. Conversely, early spring may become more suitable for spawning. BFT are therefore likely to be vulnerable to climate change, and there is potential for significant impacts on spawning and migration behaviours.

Keywords: bluefin tuna, climate change, Gulf of Mexico.

Introduction

Over the past 45 years, mean water temperatures in the upper 300 m of the oceans have increased by 0.3°C (Levitus *et al.*, 2000), and they are expected to continue increasing throughout the remaining portion of the 21st century (Hansen *et al.*, 2006; Christensen *et al.*, 2007). A warming climate will result in regional environmental changes relevant to marine ecosystems, including changes in precipitation and evaporation rates, changes in riverine discharge, loss of coastal habitat through flooding, changing oceanic circulations, and increasing ocean acidification (Scavia *et al.*, 2002; Roessig *et al.*, 2004). Within marine ecosystems, fish and fisheries are likely to be affected through the loss or degradation of nearshore fish habitat, alteration of larval dispersion pathways, and changes in species ranges, because of physiological and behavioural responses to environmental gradients (Scavia *et al.*, 2002; Perry *et al.*, 2005; Hare *et al.*, 2010). Contractions of species ranges, in both space and time, are likely to be most pronounced where species already exist near the upper limits of their physical tolerances (Pörtner and Peck, 2010).

Current climate forecasting models predict that water temperatures in the Gulf of Mexico (GOM) large marine ecosystem will be significantly affected by climate change (Christensen *et al.*, 2007). Commercial and recreational fisheries in the GOM may be affected strongly and adversely by such warming conditions and fisheries production could decrease substantially (Cheung *et al.*, 2009). The impacts of climate change are already measurable in inshore communities in the northern GOM, with shifts in nearshore fish assemblages (Fodrie *et al.*, 2009) and distributions of species, such as manatee (*Trichechus manatus*; Fertl *et al.*, 2005) and bonefish (*Albula vulpes*; Cuevas *et al.*, 2004). However, the impacts of climate change on offshore regions of the GOM and pelagic species that utilize this habitat are largely unknown.

Many large migratory fish species with high economic and ecological importance occupy the GOM during some portion of their life cycles, including the Atlantic bluefin tuna (BFT; *Thunnus thynnus*). Although this species is widely distributed, the vast majority of spawning in the western Atlantic has been recorded only in the GOM, from mid-April to June (Richards, 1976; Stokesbury *et al.*, 2004). BFT possess a unique physiology that allows them to tolerate colder waters than other tuna and has facilitated their expansion into feeding areas in the North Atlantic (Lutcavage *et al.*, 2000). Although BFT migrate long distances to reach the GOM and spawn, they may be adversely affected by warm (>28–30°C) waters (Blank *et al.*, 2004) and display behavioural patterns to avoid warm features in the GOM, such as the Loop Current (LC; Teo *et al.*, 2007a). Tagged BFT have not been recorded in ambient temperatures of >30°C and nearly 30 years of plankton surveys by NOAA Fisheries in the GOM have not collected BFT larvae at locations where sea surface temperature (SST) exceeds 29°C (Muhling *et al.*, 2010). Large BFT spawning in the GOM during late spring may therefore

be approaching the limits of their cardiac capacity (Blank *et al.*, 2004), as ambient water temperatures approach 30°C in late June.

Adult BFT are likely to target moderately warm waters to spawn. Tagged BFT in the GOM during spring preferentially inhabit waters between 24 and 27°C (Block *et al.*, 2005; Teo *et al.*, 2007b), and larvae are collected most commonly in waters of between 23.5 and 28°C (Muhling *et al.*, 2010). The lower limit of spawning activity is likely to be ~24°C (Schaefer, 2001; Masuma *et al.*, 2008), and larval BFT development is optimal at ~25°C (Miyashita *et al.*, 2000). In the Mediterranean Sea, spawning condition of adult BFT is well correlated with water temperature (Medina *et al.*, 2002; Heinisch *et al.*, 2008), and both initiation and duration of spawning are likely temperature controlled (Masuma *et al.*, 2006). If commencement of spawning requires a minimum water temperature and adult BFT cannot tolerate waters above a maximum temperature limit, a specific temperature window exists for spawning activity. It is therefore likely that shifts in water temperatures in the GOM will affect the spatial and/or the temporal distribution of BFT spawning effort. Changes in spawning times, spawning areas, and migratory behaviours are possible (Fromentin and Powers, 2005), with subsequent effects on stock sizes and fisheries.

Previous work has defined associations between larval BFT occurrences and environmental variables, especially temperature (Muhling *et al.*, 2010). This has allowed a basic classification of BFT spawning habitat within the GOM. Given their physiology, temperature-driven changes to BFT distributions or behaviours within the GOM are highly possible under climate change scenarios. To predict the likely nature of these changes, this project aimed to define current associations between BFT and temperature; then to project temporal and spatial changes in available spawning habitat over the next 100 years, using projections from an ensemble of climate models. Larval BFT occurrences were derived from plankton survey data completed under the Southeast Area Monitoring and Assessment programme (SEAMAP; 1982–2006) and adult occurrences from observer data from longline fishing vessels (1992–2009). We hypothesized that increasing temperatures in the GOM would increase the amount of theoretically suitable spawning habitat in early spring (March and April) and decrease available habitat in late spring (June).

Methods

Biological data collection

Larval BFT data were available for every year from 1982 to 2006, except 1985 and 2005, from the National Marine Fisheries Service SEAMAP. Both bongo and neuston net tows were completed across a grid of stations (the SEAMAP grid) in the northern GOM in late April and May, with sampling continuing into June in some years. Cruises were usually divided into two legs, with the grid of stations completed once on each leg. Bongo nets were fitted with 333-μm mesh, on two 61 cm diameter round frames and were towed obliquely as described in Scott *et al.* (1993) and Richards *et al.* (1993), mostly to 200 m depth. Larval fish concentrations per cubic metre of seawater sampled were calculated using the General Oceanics flowmeter fitted to the net. The neuston nets were fitted with 0.95 mm mesh on a 1 × 2 m frame and were towed at the surface. Samples from the neuston net and the right bongo net only were sorted and larvae identified to the lowest possible taxa at the Polish Plankton Sorting and Identification Center in Szczecin, Poland. The identifications of Scombridae larvae were validated at the Southeast Fisheries Science Center in Miami, FL, and occurrences of larval BFT were recorded. If >0 BFT larvae were collected at a station in either bongo or neuston nets or in both, then the station was considered "positive" for BFT larvae.

Hydrographic data were collected on plankton cruises using a Seabird SBE 9/11 Plus CTD with an SBE 03 temperature sensor, SBE digiquartz pressure sensor, SBE 04 conductivity sensor, and SBE 43 dissolved oxygen sensor. Temperatures from the surface and 200 m depth were utilized in this study.

Adult BFT were caught on longline gear in the GOM, as bycatch in fisheries targeting other species. Data from observers present on fishing vessels were available from 1992 to 2009. Unfortunately, reliable temperature data were not available concurrent with BFT catches. To roughly define the probability of catching BFT on a longline gear under GOM-wide temperature regimes, daily mean SST data were extracted from two sources: the HYCOM-NCODA GOM 1/25° Resolution Analysis (www.hycom.org) and two buoys in the western and the central GOM (Figure 1), for the date of each adult BFT catch. HYCOM surface temperature data were available from 2003 on and buoy data for 1992 on. The correlation between daily mean temperatures at the two buoys was high ($r^2 = 0.86$), suggesting that temperatures in the mid- and western GOM varied in a consistent manner. Relationships between adult BFT and extracted temperatures from HYCOM and buoys were used in combination with published temperature preferences and limits to adult physiology and behaviour to predict potential effects of climate change on distributions and spawning activity.

Definition of relationships between BFT and temperature

Relationships between the occurrences of BFT larvae and adults with SST and day of the year (within spring to early summer) were initially investigated using simple preference models (Cock, 1978). The proportion of stations (larvae) or sets (adults) containing BFT were calculated across a range of temperatures and dates. This allowed an examination of whether either larvae or adults were proportionally more likely to be caught at certain temperatures, or around certain dates.

To define statistically associations between larval BFT occurrences and water temperature, a classification-tree model was constructed, using DTREG software (Sherrod, 2003). Classification-tree modelling splits a dataset into increasingly small and homogeneous subsets, with each split made using the variable that provides the greatest improvement in the homogeneity of the two resulting groups (De'ath and Fabricius, 2000; Castellon and Sieving, 2006). The classification-tree approach was suited to our dataset as it is a non-parametric procedure that can cope with non-linear relationships and interaction among predictor variables (Franklin, 1998; De'ath and Fabricius, 2000; Vayssieres *et al.*, 2000). A misclassification cost can also be set that is useful for predicting the occurrence of sparsely distributed organisms, such as larval fish. The tree constructed here was a simplification of a previous study (Muhling *et al.*, 2010) that predicted the occurrence of larval BFT using a variety of *in situ* variables, such as temperature, salinity, and settled plankton volumes. To increase the predictive power of the initial classification tree, stochastic gradient boosting was

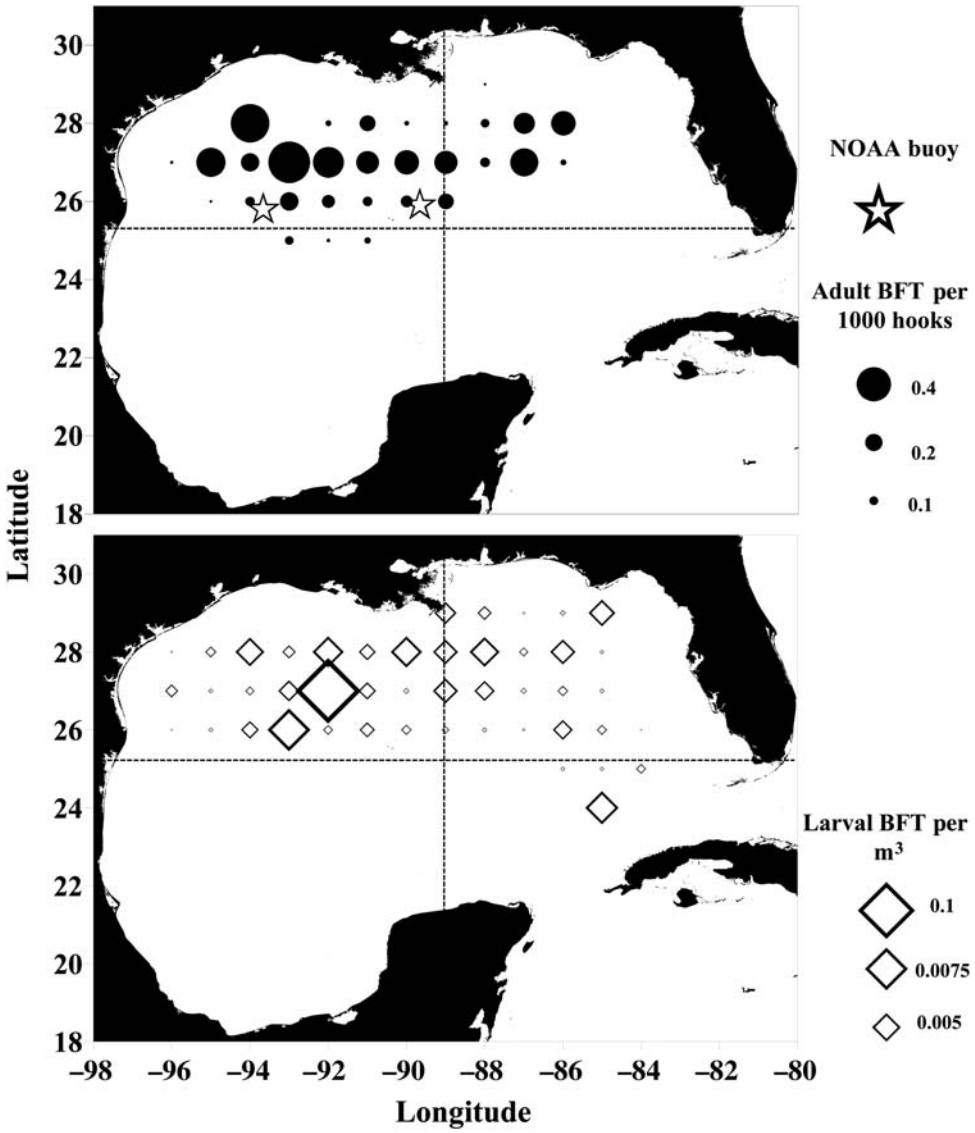

Figure 1. Mean catches of adult BFT per 1000 hooks on longline fishing vessels, 1992 to 2009, per whole latitude and longitude degree (top) and mean catches of larval BFT per m^3 of seawater sampled, 1982–2006 (bottom). Positions of two NOAA buoys used to provide temperature data and the four zones of the GOM (northwest, northeast, southwest, and southeast) are also illustrated.

employed. This technique is an adaptive method that combines several smaller tree models after the initial classification tree to improve predictive performance. It is a highly accurate habitat modelling technique, comparable with methods such as generalized additive models (Elith *et al.*, 2008). This analysis aimed to define habitat conditions that had the highest likelihood of occurrence of BFT larvae, using only water temperature at the surface and at 200 m depth.

Water temperature at 200 m depth does not tend to change seasonally; it therefore provides a good indicator of water mass and is useful for displaying the boundary of the LC and warm eddies (Wennekens, 1959). Water temperature is also known to initiate spawning (Schaefer, 2001), and the very warm water found in the GOM in late spring and summer is close to the physiological limit of adult BFT (Blank *et al.*, 2004). Associations defined between temperatures at the surface and at depth and BFT in the 20th century should therefore retain some reliability for projections of future scenarios.

Climate models

An ensemble of 20 models was used to predict temperature changes within the GOM to the end of the 21st century, under scenario A1B, for the months of March, April, May, and June (Table 1). Scenario A1B is characterized by a rapid and successful economic growth, the development of new and efficient technologies, and a balanced emphasis on the use of fossil and non-fossil fuel sources, and is the scenario best represented in recent literature (Nakicenovic and Swart, 2000). Data from each model were interpolated to a 0.25° resolution to allow comparison with observed climatology data for the past 30 years of the 20th century, which were sourced from the Generalized Digital Environmental Model version 3.0 (GDEM3) temperature and salinity climatology (Carnes, 2009).

Predictions from each climate model were weighted to give the most accurate models greater input into the final ensemble mean. To achieve this, the square root of the difference between the

Table 1. Suite of 20 climate models used in the prediction of future temperatures in the GOM.

Climate model	Institution	Weight
BCCR-BCM 2.0	Bjerknes Centre for Climate Research, University of Bergen, Norway	0.52
CNRM-CM3	Centre National de Recherches Météorologiques, Météo France, France	0.40
GISS-AOM	Goddard Institute for Space Studies (GISS), NASA, USA	0.34
GISS-EH	Goddard Institute for Space Studies (GISS), NASA, USA	0.61
GISS-ER	Goddard Institute for Space Studies (GISS), NASA, USA	1.33
IAP-FGOALS-g 1.0	LASG, Institute of Atmospheric Physics, Chinese Academy of Sciences, Beijing, China	1.02
INGV-ECHAM-4	Instituto Nazionale di Geofisica e Vulcanologia, Italy	2.89
MIROC 3.2(medres)	Center for Climate System Research (The University of Tokyo), National Institute for Environmental Studies and Frontier Research Center for Global Change (JAMSTEC), Japan	0.63
CGCM3.1	Canadian Centre for Climate Modelling and Analysis, Canada	0.83
CGCM3.1(T63)	Canadian Centre for Climate Modelling and Analysis, Canada	0.60
CSIRO-Mk 3.0	CSIRO Atmospheric Research, Australia	0.11
CSIRO-Mk 3.5	CSIRO Atmospheric Research, Australia	3.15
GFDL-CM 2.0	US Department of Commerce/NOAA/ Geophysical Fluid Dynamics Laboratory, USA	0.57
GFDL-CM 2.1	US Department of Commerce/NOAA/ Geophysical Fluid Dynamics Laboratory, USA	0.74
IPSL-CM4	Institut Pierre Simon Laplace, France	0.30
ECHO-G	Meteorological Institute of the University of Bonn, Germany and Meteorological Research Institute of KMA, Korea	0.82
ECHAM5/ MPI-OM	Max Planck Institute for Meteorology, Germany	1.54
MRI-CGCM 2.3.2	Meteorological Research Institute, Japan	2.80
CCSM3	National Center for Atmospheric Research, USA	0.79
PCM	National Center for Atmospheric Research, USA	0.01

The weight of each model, as determined by its ability to hindcast water temperature in the GOM for the late 20th century (1971–1999), is also presented.

predicted (modelled) and observed (GDEM) temperatures for the past 30 years of the 20th century and the observed temperatures from GDEM was calculated for all grid points in the GOM. The root mean square (RMS) error was then calculated using the following equation:

$$\mathrm{RMS}(i) = \sqrt{\frac{1}{m}\sum_{i=1}^{m}(T_{\mathrm{model}}(i) - T_{\mathrm{obs}})^2}, \quad (1)$$

where i is the model number and m the grid point. RMS values are calculated for surface, 100 m, and 200 m temperatures. The weight

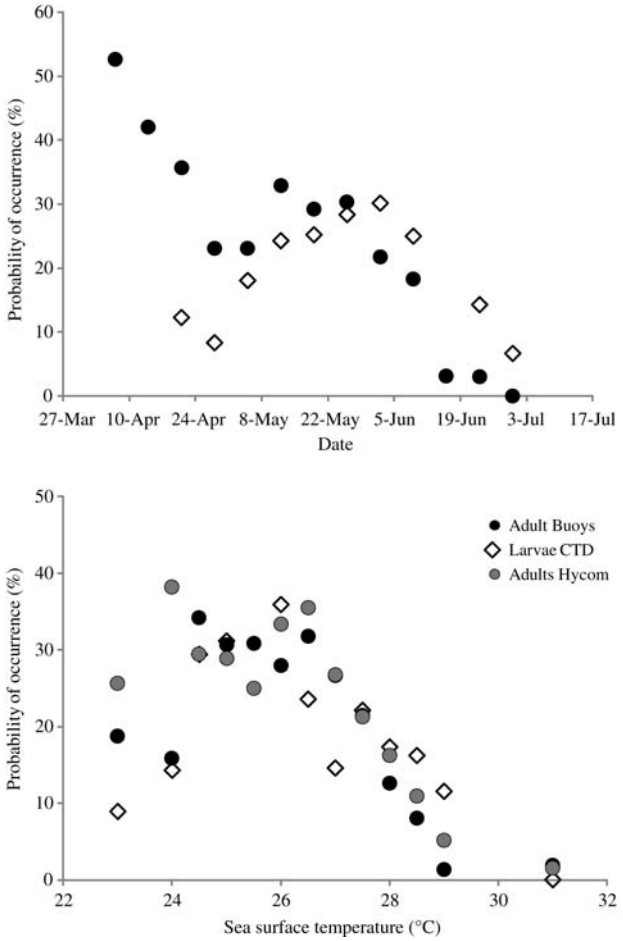

Figure 2. Probability of occurrence of adult and larval BFT across a range of dates (top) and surface water temperatures (bottom) in the GOM in spring. Temperatures associated with adult catches were derived from the HYCOM-NCODA GOM 1/25° Resolution Analysis and from buoys; temperatures associated with larval catches were derived from CTD casts.

for each model is computed based on the following equation:

$$\mathrm{weight}\ (i) = \beta\left(\frac{e^{-\left(\frac{\mathrm{RMS}_0(i)}{L_0}\right)^2} + e^{-\left(\frac{\mathrm{RMS}_{100}(i)}{L_{100}}\right)^2} + e^{-\left(\frac{\mathrm{RMS}_{200}(i)}{L_{200}}\right)^2}}{3}\right), \quad (2)$$

and

$$\beta = \frac{N}{\sum_{i=1}^{n}\{(e^{-(\mathrm{RMS}_0(i)/L_0)^2} + e^{-(\mathrm{RMS}_{100}(i)/L_{100})^2} + e^{-(\mathrm{RMS}_{200}(i)/L_{200})^2})/3\}},$$

where N is the number of models, and L_0, L_{100}, L_{200} are the tolerances to be chosen for the surface, 100 m, and 200 m temperatures. All tolerances (L_0, L_{100}, L_{200}) were set to 1°C, meaning that no weight was given to models with >1°C of RMS error.

Because many of the models displayed a large bias in their predictions of temperature before a weighting coefficient was applied, the projected change in temperature displayed by each model for each decade was added to the observed GDEM 20th century data before applying a weighting coefficient. The same weight

was given to temperature predictions at the surface, 100 and 200 m.

A weighted mean of temperature at the surface and at 200 m, across the GOM, was then predicted for each decade of the 21st century, from 2005 to 2015. These data were then run using the classification-tree model that was built using observed larval BFT data from the 20th century. Each grid point in the GOM (at 0.25° resolution) for each decade was scored with a probability that larval BFT would be present under projected temperature conditions and displayed as a surface using kriging. Although projections were made across the GOM, available biological data existed only for the northern GOM, within US waters. Predictions of habitat in the southern GOM should therefore be considered untested. The potential gain or loss of spawning habitat was quantified using the changes in probability of larval BFT occurring at each grid point across the GOM to the end of the 21st century.

Because few data were available on direct preferences of adult BFT for waters of specific temperatures, published temperature limits on BFT spawning behaviour and thermoregulatory abilities were employed to classify the GOM into favourable and unfavourable habitat for spawning. The lower limit for BFT spawning has been consistently recorded as ~24°C (Schaefer, 2001), and it was therefore assumed that although adult BFT would not be excluded from waters below this temperature, spawning was not likely. Tagged BFT in the GOM in spring have been demonstrated to prefer areas with SSTs between 24 and 27°C (Teo *et al.*, 2007b) and waters of ~25°C have been suggested as most advantageous for the development of larval Pacific BFT (Miyashita *et al.*, 2000). Although spawning takes place in slightly cooler waters in the Mediterranean, Garcia *et al.* (2005) also found an association between larval BFT and temperature, with larvae most likely to be collected where SSTs were between 24 and 25°C. A temperature of 30°C was considered the upper physiological limit of adult BFT (Blank *et al.*, 2004), and neither adult nor larval BFT have been recorded in waters above this temperature (Block *et al.*, 2005; Muhling *et al.*, 2010). Waters of between 27 and 30°C are likely to be warmer than preferred by adult BFT. However, their physiological and behavioural responses to moderately warm waters in this range are unknown.

Results

Relationships between adult and larval BFT and temperature

Both adult and larval BFT were distributed across the GOM, although adult abundances were higher in the west (Figure 1). Adult BFT were more likely to be caught near 27°N, whereas larvae were more widespread in their latitudinal distribution.

Occurrences of both adult and larval BFT were correlated with day of the year and SST (Figure 2). Adult BFT were abundant in early spring, became rarer in early June and were absent by the end of June. In contrast, the proportion of sampled stations containing BFT larvae increased from late April to the end of May, before catches decreased in June. Both adult and larval BFT were most likely to be collected where SSTs were between ~24 and 28°C and were rarely caught when SSTs exceeded 29°C. Adult temperature preference curves derived using the HYCOM model and buoy data were similar, although preferences in cooler waters were higher when calculated with extracted HYCOM data.

A simple classification-tree model (Figure 3), with a misclassification cost of 5:1, placed 88.7% (205 of 231) BFT larvae in theoretically suitable habitat, as defined by temperature at the surface and at 200 m. Larvae were more likely to be collected where

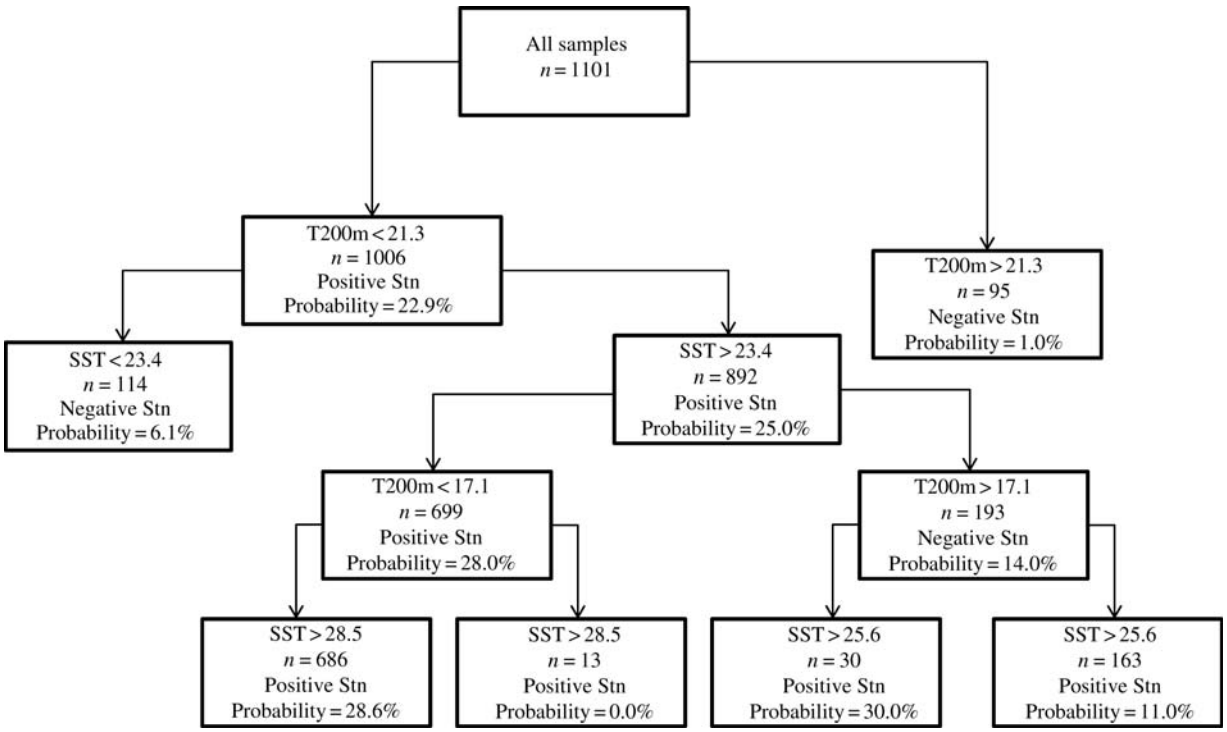

Figure 3. Classification-tree model for predicting the presence or the absence of BFT larvae in the northern GOM, given temperature at the surface and at 200 m. The number of samples at each node is displayed, as is the probability of occurrence of BFT larvae.

temperatures at 200 m were lower than 21.3°C and where SSTs were between 23.4 and 28.5°C (Figure 3). Stochastic gradient boosting improved the accuracy of the model to 96.2%. Relationships defined between both larval and adult BFT and water temperatures therefore agreed well with published preferences from larval surveys and behaviour of tagged adults (Teo *et al.*, 2007a; Muhling *et al.*, 2010).

Projected changes in the physical environments of the GOM

The upper ocean of the GOM, along with the Caribbean Sea, serves as an important contributor to the Atlantic Warm Pool (AWP), which is a warm body of surface water (>28.5°C) in the tropical North Atlantic. The AWP releases large amounts of moisture into the overlying atmosphere and hence influences rainfall over the continental United States and Central America, as well as Atlantic hurricane activity (Wang *et al.*, 2006; Wang and Lee, 2007). The upper ocean of the GOM undergoes warming during the BFT spawning months of April to June and cooling in other months. During winter, the GOM upper ocean experiences intense cooling at the surface, because of frequent mid-latitude frontal passages and an associated increase in latent cooling. Therefore, the shortwave radiation and the latent heat flux are the major forcing terms that drive the seasonal cycle of upper ocean heat budget in the GOM (Lee *et al.*, 2005, 2007).

The GOM-averaged SST evolution for each calendar month for the period of 2001 and 2098 obtained from the ensemble average of all IPCC-AR4 climate model simulations under the A1B scenario is illustrated in Figure 4. In the earlier period of the 21st century, the AWP appeared during July to September (Enfield and Lee, 2005; Lee *et al.*, 2005, 2007), whereas towards the end of the 21st century, the AWP appeared much earlier in late May to early June and disappeared in late October to early November. As a result, the preferred period for BFT spawning (~24–27°C) was shifted from late April to early June in the early 21st century to mid-March to late April in the late 21st century.

To have a better perspective of what may cause the SST increase in the GOM, the GOM-averaged surface heat flux components, namely shortwave radiation, long-wave radiation, sensible heat flux, latent heat flux, and the net surface heat flux, were plotted using the ensemble average of all IPCC-AR4 climate model simulations under the SRESA1B scenario as illustrated in Figure 5. For each surface heat flux component, except for the net surface heat flux, the average of 2001–2010 was subtracted for a better visual comparison. As expected, the increased greenhouse gas concentrations induced a steady increase in the downward long-wave radiation. Although much weaker than the long-wave radiation

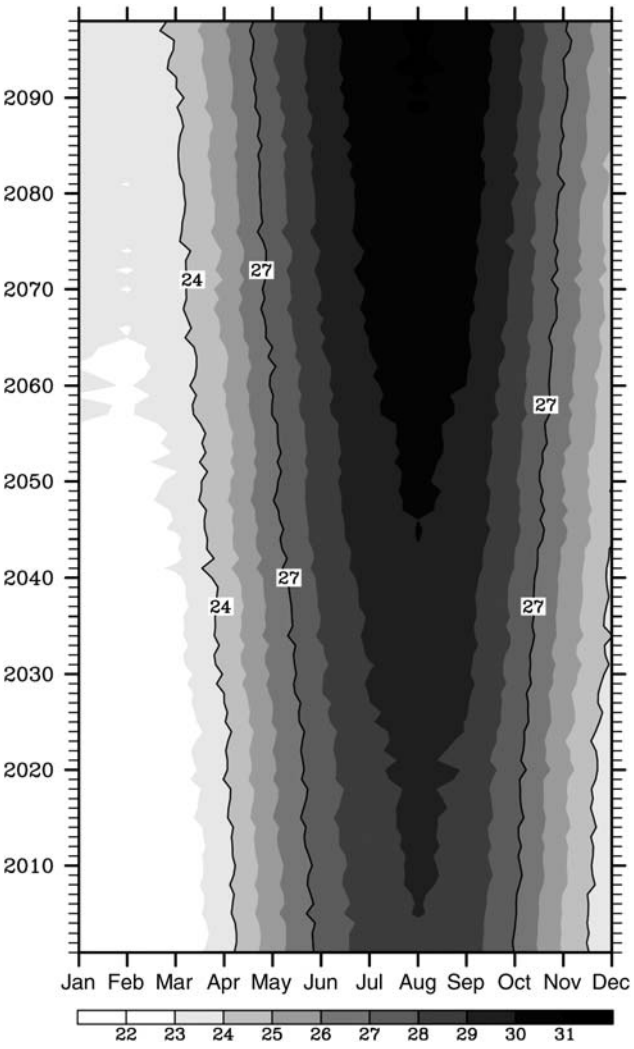

Figure 4. The GOM-averaged SST evolution for each calendar month for the period of 2001 and 2098 obtained from the ensemble average of all IPCC-AR4 climate model simulations under SRESA1B scenario. Note that the preferred period for BFT spawning (~24–27°C) is shifted from late April to early June in the early 21st century to mid-March to late-April in the late 21st century.

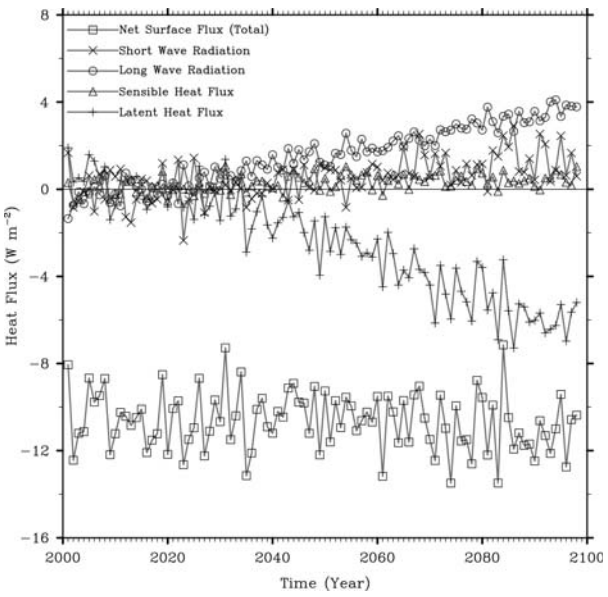

Figure 5. The GOM-averaged surface heat flux components, namely shortwave radiation, long-wave radiation, sensible heat flux, latent heat flux, and net surface heat flux, obtained from the ensemble average of all IPCC-AR4 climate model simulations under SRESA1B scenario. For each surface-heat-flux component except net surface heat flux, the average of 2001–2010 is subtracted for better visual comparison.

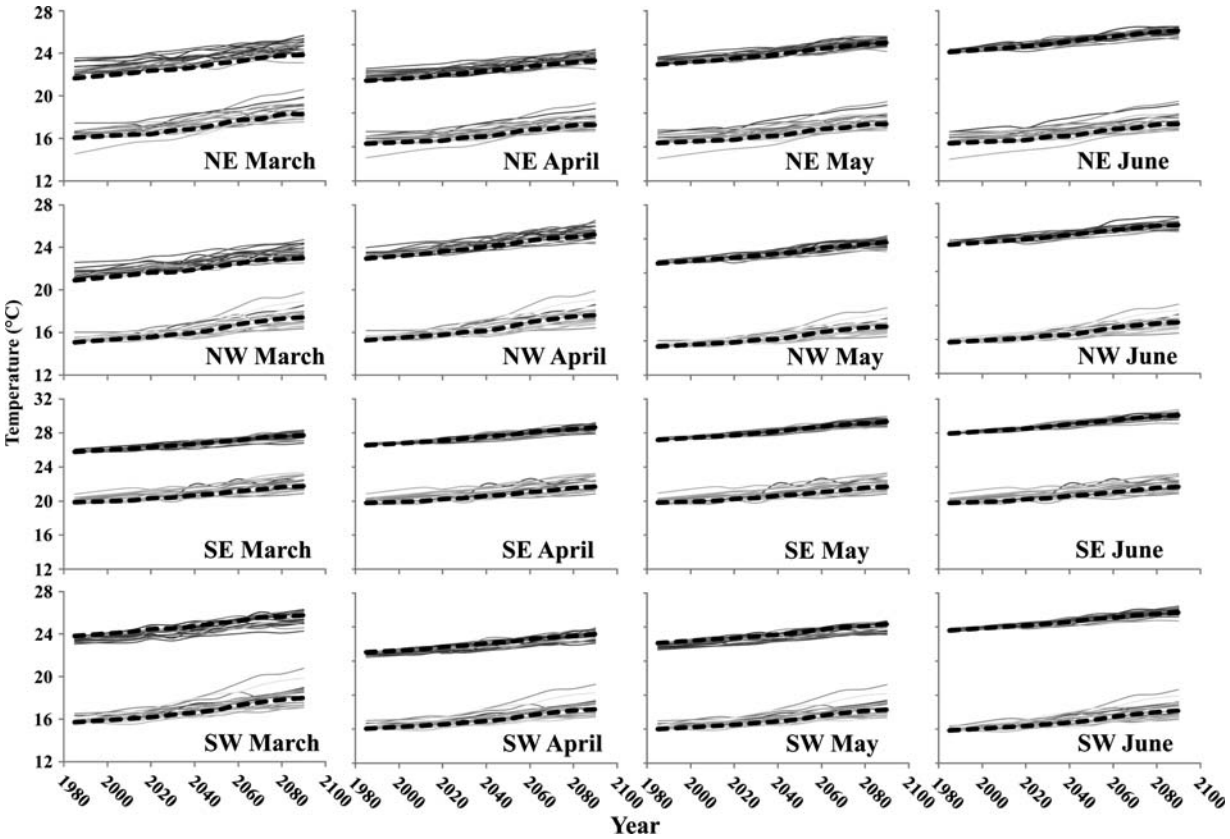

Figure 6. Prediction of temperature for four zones of the GOM, for the months of March, April, May, and June. Projections from all 20 models are displayed, with the weighted mean as the heavy dashed line. Each plot displays projections for water temperature at the surface (top series) and 200 m (bottom series).

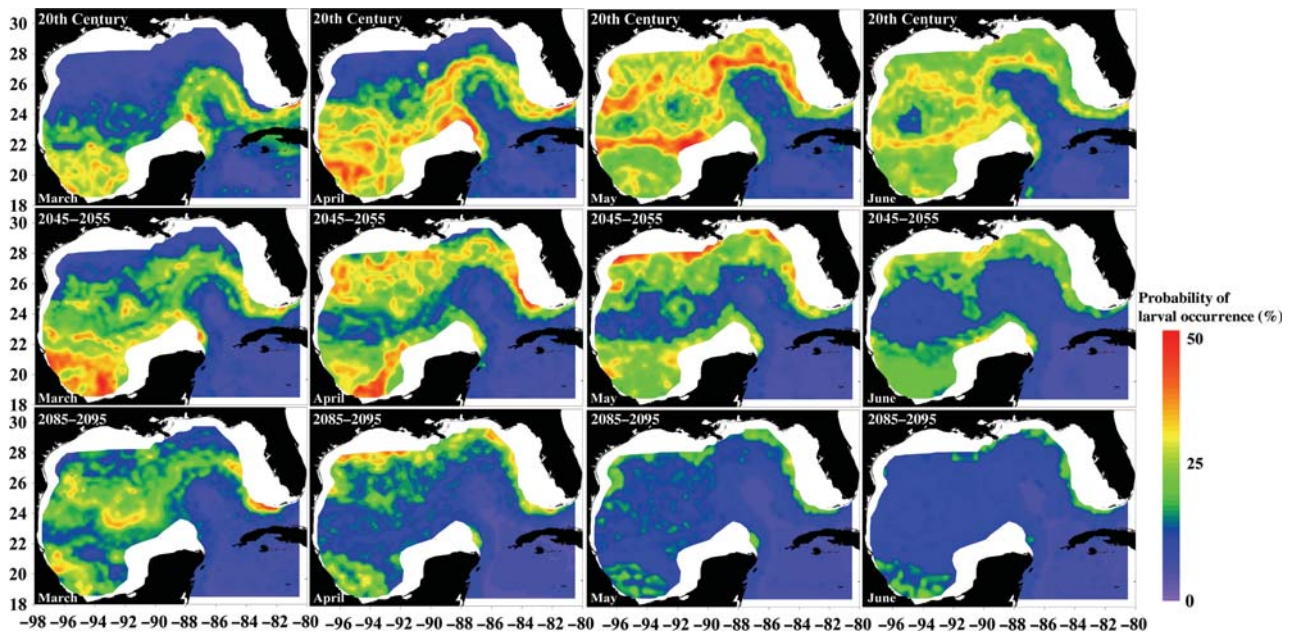

Figure 7. Prediction of the extent of habitat suitable for the occurrence of larval BFT in the GOM under late 20th century conditions (1971–1999) and projected conditions in 2045–2055 and 2085–2095, for the months of March, April, May, and June. The probability of occurrence (%) is illustrated, based on output from the boosted classification-tree model using weighted mean temperature values.

component, the short-wave radiation also increased over time, suggesting that precipitation rate and cloud cover were both reduced over the GOM. It is likely that the increased SST over the GOM contributed to the increased latent cooling. The (total) net surface heat flux was negative overall, suggesting that ocean dynamics play a role in warming the upper ocean of the GOM.

To formulate data for inclusion in the larval habitat model, a weighted mean of temperature at the surface and at 200 m was predicted using the ensemble projections from all climate models for each grid point in the GOM, for the months of March, April, May, and June. For simplicity, a mean value for the northeast, northwest, southeast, and southwest GOM was displayed for each model and for each decade (Figure 6). Overall, model projections suggested a mean increase of 2.10°C across the GOM (mean 95% CI ±0.10°C) at the surface and 2.15°C (95% CI ±0.15°C) at 200 m, by 2085–2095, compared with the late 20th century values. However, mean water temperatures at the surface and at 200 m were variable among models. The models predicting the greatest increases in temperature were usually those that overestimated 20th century temperatures by the greatest amount. These models therefore had a lower weighting, contributing less to the weighted mean. As a result, the weighted mean was often closest to the model predicting cooler temperatures. This was especially the case in March and April (Figure 6). Projected temperatures at 200 m were particularly variable in the southeastern GOM, within the zone where the LC would have the greatest influence.

Spatial and temporal changes in larval BFT distributions

Data for each grid point in the GOM for each decade and each month were run using the boosted classification-tree model and scored through the weighted mean prediction of temperature at the surface and at 200 m as variables. The output was a probability of larval BFT occurrence at each location, for each month in each decade. When interpolated, these probabilities gave an estimation of potentially favourable habitat for larval BFT in the GOM (Figure 7). Scenarios are displayed for the end of 20th century, from GDEM, the middle of the 21st century (2045–2055) and the end of the 21st century (2085–2095), for March, April, May, and June. Under 20th century conditions, the habitat likely to support BFT larvae tended to be located in the southern GOM in March and April and across most of the GOM in May and June. By 2045 to 2055, the suitable habitat had moved northwards in March and April, but had started to shrink in the mid-latitudes of the GOM in April. The proportion of the GOM where probabilities of collecting larval BFT were predicted to be low increased throughout May and June. By 2085–2095, the favourable habitat remained extensive in March, but was much reduced in April, May, and June.

The proportion of grid points in the suitable habitat (>20% probability of larval occurrence) increased by 62% in March and 2% in April by 2050, although decreasing 39% in May and 61% in June (Figure 8). By 2090, the suitable habitat had increased by 20% in March, but decreased by 66% in April, 93% in May, and 96% in June. Areas of unsuitable habitat (<10% probability of larval occurrence) decreased by 21% in March, but increased by 52% in April, 206% in May, and 334% in June by 2090. Overall, the total suitable habitat across the 4-month spawning season decreased from 44% of grid points in the late 20th century to 12% by the end of the 21st century.

Predictions of the effects of climate change on adult BFT distributions were more difficult to make, because direct relationships between adult BFT and temperature in the GOM are scarce. However, a simplistic approach with four categories of suitability was created, based upon projected SST in the GOM (Figure 9). The potential suitability of March for spawning increased throughout the 21st century, with most of the GOM moving into a suitable temperature range by 2085–2095. The cooler waters currently found in the northern GOM in April were predicted to disappear by the end of the 21st century, although the rest of the GOM was predicted to remain within the 24–27°C range in this month (Figure 9). In May, the GOM was predicted to shift from being largely in 24–27°C water to 27–30°C water by 2095. In June, most of the GOM was projected to become very warm by the end of the century, approaching physiological limits for adult BFT (30°C), especially in southeastern areas where BFT enter and exit the GOM. These patterns displayed some similarity to the predictions of larval habitat, with a potential increase in the suitability of March, some warming-induced habitat loss in April by 2095, and more conspicuous loss of suitable habitat in May and June across the GOM.

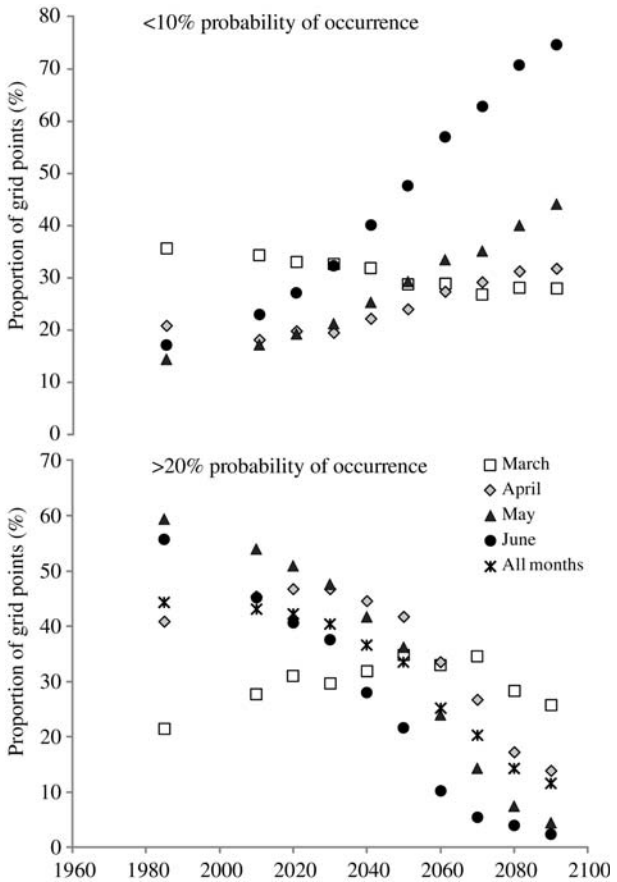

Figure 8. Temporal trends in the number of grid points across the GOM that were predicted to have a <10% (top) or >20% (bottom) chance of containing BFT larvae, based on output from the boosted classification-tree model using weighted mean temperature values.

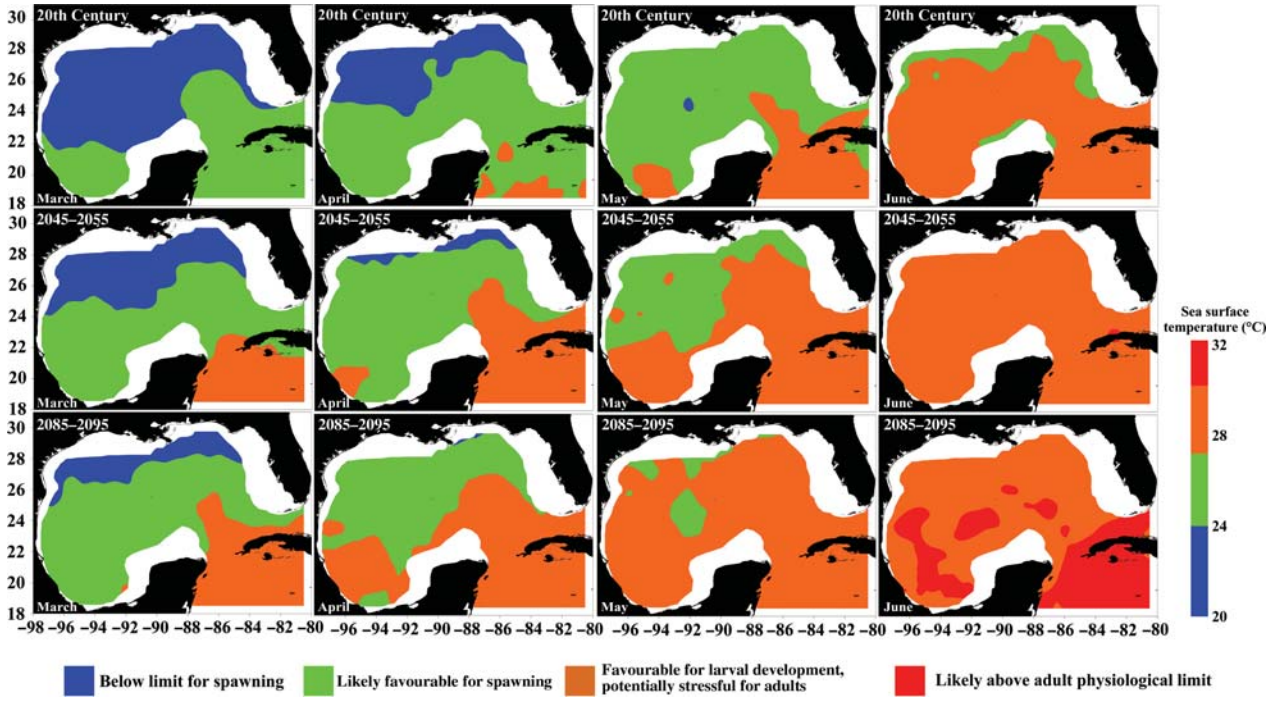

Figure 9. Predicted suitability of habitat in the GOM for adult BFT, based on SSTs in the late 20th century (1971–1999) and projected conditions in 2045–2055 and 2085–2095. Categories were estimated based on the published associations between temperature and BFT spawning and physiology.

Discussion

Data presented in this study support published evidence of BFT migration and spawning behaviour, with larvae collected from mid-April to mid-June and neither larvae nor adults found in association with ambient water temperatures of >29°C. Adult BFT generally migrate to the GOM from northern Atlantic feeding grounds between December and June (Block *et al.*, 2005), although this may not be an annual occurrence for all individuals (Lutcavage *et al.*, 1999). Spawning commences in April and is likely to be triggered by temperature; a minimum threshold, minimum rate of change, or both (Masuma *et al.*, 2006; Heinisch *et al.*, 2008). BFT are likely to be serial spawners and may not stay in the GOM throughout the entire spawning season (Farley and Davis, 1998; Block *et al.*, 2001; Rooker *et al.*, 2007). However, by late June, most BFT have left the GOM (Teo *et al.*, 2007a), probably in association with rising ambient water temperatures.

Initial climate modelling results presented here displayed an increase in water temperatures at the surface and at depth, in the GOM during the current BFT spawning season. Model projections were highly variable; however, they suggest that an increase in water temperatures of ~2.0°C down to 200 m depth could be expected under emission scenario A1B. Under these conditions, suitable spawning habitat for BFT in the GOM would increase in March, initially increase slightly, then decrease in April and be substantially reduced in May and June. These results partly supported the original hypothesis of an improvement in spawning conditions in early spring, but it appears that water temperatures may warm to the extent that both April and May will be largely unsuitable for spawning by the end of the 21st century.

Global climate change therefore has high potential for affecting temporal and spatial patterns of BFT spawning activity in the GOM. If spawning activity is indeed triggered by temperature and GOM waters warm earlier in the year, then spawning may commence sooner and finish sooner. Some fish species also commence spawning in association with photoperiod (Carrillo *et al.*, 1989); if this is the case for BFT, the spawning season could instead be prematurely truncated.

Although the precise reasons for BFT migrating large distances to spawn in the GOM remain unclear, it is likely that warm, oligotrophic waters benefit larval survival. Larval growth rates are high in warm water (Brothers *et al.*, 1983; Miyashita *et al.*, 2000) and oligotrophic waters may present favourable feeding conditions for larvae with specialized diets (Bakun, 2006; Llopiz *et al.*, 2010). Under climate change conditions, primary and secondary productivity regimes could be altered (Polovina *et al.*, 2007) and the current "match" between suitable water temperatures and low productivity in the open GOM in spring (Muller-Karger *et al.*, 1991) might not be maintained. If this is the case, then the survival rates of BFT larvae may change, as concentrations of planktonic prey and predators change. Increasing water temperatures will therefore affect spawning times and locations, larval growth, feeding, and survival. However, trophic relationships of this nature are complex and assessment of ecosystem-scale effects of climate change on the GOM require far more sophisticated models than those used in this study.

Historical data from the Mediterranean Sea suggest that BFT may change their migration routes and spawning behaviours in association with long-term fluctuations in temperature (Ravier and Fromentin, 2004). Migration rates and routes of BFT may also be influenced by prey concentrations on their feeding and spawning grounds (Polovina, 2007). The currently accepted paradigm is that two stocks of Atlantic BFT with shared feeding grounds in the North Atlantic spawn in only two areas (the

GOM and Mediterranean Sea). However, fisheries have existed for BFT in the past in other areas, such as Brazil (Fonteneau, 2009) and the North Sea (Fromentin, 2009). Both fisheries disappeared in the 1950–1960s, although the importance of contributing factors, such as environmental change, changes in migration rates, and fishing pressure are not well understood. This may suggest more plasticity in feeding grounds and perhaps spawning grounds than is currently assumed. However, if climate change and warming water result in reduced suitability of the GOM for BFT spawning, a major behavioural change would be required if a new spawning ground were to be colonized. The ability of BFT to adapt in this manner is unknown. BFT have been heavily exploited in the past and are currently classified as overfished, with stocks at low levels compared with 30–40 years ago (Rooker *et al.*, 2007; McAllister and Carruthers, 2008). If overfishing has reduced genetic diversity, the ability of the species to adapt to climate change may have been compromised (Perry *et al.*, 2010; Planque *et al.*, 2010).

The results presented here are preliminary in the investigation of climate change effects on BFT, and hence discussion of implications for BFT under climate change scenarios could be considered speculative. One source of such uncertainty is from the IPCC-AR4 climate models. These models have typical spatial resolution of ~1°; they therefore have a limited ability to resolve the regional western boundary current system (i.e. Yucatan Current, LC, and Florida Current), which likely has a significant impact on the heat budget cycle of the GOM. A high-resolution model simulation is required for a detailed and reliable assessment of the impact of ocean dynamics. IPCC-AR4 climate models suggest that the GOM current system may slow down because of the projected reduction of the Atlantic thermohaline circulation. However, it is unclear whether and how the reduced ocean current system will interact with the projected surface warming in the GOM. Related to this issue of model uncertainty, IPCC-AR4 climate models project that the rainfall over the GOM may be reduced. Therefore, the surface salinity of the GOM should increase. However, we found that none of the 20 climate models considered in this study could reproduce the 20th century upper ocean salinity of the GOM. Therefore, we decided not to include salinity in our analysis. Downscaling of climate models to the regional scale of the GOM will be essential for resolving such model uncertainty issues.

In summary, further research is required on ecosystem-based responses to climate change in the GOM and other large marine ecosystems, before conclusions that are more robust can be drawn. However, this study suggests that BFT are likely to be vulnerable to climate change impacts and that the potential for significant impacts on spawning and migration is high. If this species is to be managed effectively under climate change conditions, improved understanding of both species responses and ecosystem-level changes is urgently needed.

Acknowledgements

We thank K. Keene and M. Schirripa from the NOAA-National Marine Fisheries Service Southeast Fisheries Science Center, and D. Enfield from the NOAA Atlantic Oceanographic and Meteorological Laboratory for provision of fisheries observer data and helpful initial discussions. We also acknowledge staff at the NOAA-NMFS Pascagoula laboratory for valuable assistance with larval fish data collection and provision, including W. Ingram, J. Lyczkowski-Schultz, K. Williams, D. Drass, D. Hanisko, and G. Zapfe. We thank all staff at the Polish Plankton Sorting and Identification Center in Szczecin, Poland, including M. Konieczna and L. Ejsymont, and extend our gratitude to the captains and crew of all the NOAA ships who collected data on the SEAMAP cruises and the fisheries observers who collected data on longline vessels. This work was partly funded by a Fisheries and the Environment (FATE) grant. The manuscript was substantially improved by comments from anonymous reviewers and the editor and we thank them for their time and efforts.

References

Bakun, A. 2006. Wasp-waist populations and marine ecosystem dynamics: navigating the "predator pit". Progress in Oceanography, 68: 271–288.

Blank, J. M., Morrissette, J. M., Landeira-Ferandez, A. M., Blackwell, S. B., Williams, T. D., and Block, B. A. 2004. *In situ* cardiac performance of Pacific bluefin tuna hearts in response to acute temperature change. Journal of Experimental Biology, 207: 881–890.

Block, B. A., Dewar, H., Blackwell, S. B., Williams, T. D., Prince, E. D., Farwell, C. J., Boustany, A., *et al.* 2001. Migratory movements, depth preferences and thermal biology of Atlantic bluefin tuna. Science, 293: 1310–1314.

Block, B. A., Teo, S. L. H., Walli, A., Boustany, A., Stokesbury, M. J. W., Farwell, C. J., Weng, K. C., *et al.* 2005. Electronic tagging and population structure of Atlantic bluefin tuna. Nature, 434: 1121–1127.

Brothers, E. B., Prince, E. D., and Lee, D. W. 1983. Age and growth of young-of-the-year bluefin tuna, *Thunnus thynnus*, from otolith microstructure. *In* Proceedings of the International Workshop on Age Determination of Oceanic Pelagic Fishes: Tunas, Billfishes and Sharks, pp. 49–59. Ed. by E. D. Prince, and L. M. Pulos. NOAA Technical Report NMFS, 8.

Carnes, M. R. 2009 Description and Evaluation of GDEM-V 3.0. Naval Research Laboratory, Stennis Space Center, NRL/MR/7330-09-9165, 6 February 2009.

Carrillo, M., Bromage, N., Zanuy, S., Serrano, R., and Prat, F. 1989. The effects of modifications in photoperiod on spawning time, ovarian development and egg quality in the sea bass (*Dicentrarchus labrax* L.). Aquaculture, 81: 351–365.

Castellon, T. D., and Sieving, K. E. 2006. Landscape history, fragmentation, and patch occupancy: models for a forest bird with a limited dispersal. Ecological Applications, 16: 2223–2234.

Cheung, W. W. L., Lam, V. W. Y., Sarmiento, J. L., Kearney, K., Watson, R., Zeller, D., and Pauly, D. 2009. Large-scale redistribution of maximum fisheries catch potential in the global ocean under climate change. Global Change Biology, 16: 24–35.

Christensen, J. H., Hewitson, B., Busculoc, A., Chen, A., Gao, X., Held, I., Jones, R., *et al.* 2007. Regional climate projections. *In* Climate Change 2007: the Physical Science Basis. Contribution of Working Group I to the Fourth Assessment Report of the Intergovernmental Panel on Climate Change. Ed. by S. Solomon, D. Qin, M. Manning, Z. Chen, M. Marquis, K. B. Avery, and H. L. Miller. Cambridge University Press, Cambridge, UK, and New York, NY, USA.

Cock, M. J. W. 1978. The assessment of preference. Journal of Animal Ecology, 47: 805–816.

Cuevas, K. J., Franks, J. S., and Buchanan, M. V. 2004. First record of bone-fish, *Albula vulpes*, from Mississippi coastal waters. Gulf and Caribbean Research, 17: 69–94.

De'ath, G., and Fabricius, K. E. 2000. Classification and regression trees: a powerful yet simple technique for ecological data analysis. Ecology, 81: 3178–3192.

Elith, J., Leathwick, J. R., and Hastie, T. 2008. A working guide to boosted regression trees. Journal of Animal Ecology, 77: 802–813.

Enfield, D. B., and Lee, S-K. 2005. The balance of the Western Hemisphere Warm Pool. Journal of Climate, 18: 2662–2681.

Farley, J. H., and Davis, T. L. O. 1998. Reproductive dynamics of southern bluefin tuna, *Thunnus maccoyii*. Fishery Bulletin US, 96: 223–236.

Fertl, D., Schiro, A. J., Regan, G. T., Beck, C. A., Adimey, N., Price-May, L., Amos, A., *et al.* 2005. Manatee occurrence in the northern Gulf of Mexico, west of Florida. Gulf and Caribbean Research, 17: 69–94.

Fodrie, F. J., Heck, K. L., Powers, S. P., Graham, W. M., and Robinson, K. L. 2009. Climate-related, decadal-scale assemblage changes in seagrass-associated fishes in the northern Gulf of Mexico. Global Change Biology, 16: 48–59.

Fonteneau, A. 2009. Atlantic bluefin tuna: 100 centuries of fluctuating fisheries. ICCAT Collective Volume of Scientific Papers, 63: 51–68.

Franklin, J. 1998. Predicting the distribution of shrub species in southern California from climate and terrain-derived variables. Journal of Vegetation Science, 9: 733–748.

Fromentin, J-M. 2009. Lessons from the past: investigating historical data from bluefin tuna fisheries. Fish and Fisheries, 10: 197–216.

Fromentin, J-M., and Powers, J. E. 2005. Atlantic bluefin tuna: population dynamics, ecology, fisheries and management. Fish and Fisheries, 6: 281–306.

Garcia, A., Alemany, F., Velez-Belchi, P., Lopez Jurado, J. L., Cortes, D., de la Serna, J. M., Gonzalez Pola, C., *et al.* 2005. Characterization of the bluefin tuna spawning habitat off the Balearic Archipelago in relation to key hydrographic features and associated environmental conditions. ICCAT Collective Volume of Scientific Papers, 58: 535–549.

Hansen, J., Sato, M., Ruedy, R., Lo, K., Lea, D. W., and Medina-Elizade, M. 2006. Global temperature change. Proceedings of the National Academy of Sciences of the USA, 103: 14288–14293.

Hare, J. A., Alexander, M. A., Fogarty, M. J., Williams, E. H., and Scott, J. D. 2010. Forecasting the dynamics of a coastal fishery species using a coupled climate-population model. Ecological Applications, 20: 452–464.

Heinisch, G., Corriero, A., Medina, A., Abascal, F. J., de la Serna, J-M., Vassallo-Agius, R., Ríos, A. B., *et al.* 2008. Spatial–temporal pattern of bluefin tuna (*Thunnus thynnus* L. 1758) gonad maturation across the Mediterranean Sea. Marine Biology, 154: 623–630.

Lee, S-K., Enfield, D. B., and Wang, C. 2005. Ocean general circulation model sensitivity experiments on the annual cycle of the Western Hemisphere Warm Pool. Journal of Geophysical Research, 110. doi:10.1029/2004JC002640.

Lee, S-K., Enfield, D. B., and Wang, C. 2007. What drives seasonal onset and decay of the Western Hemisphere Warm Pool? Journal of Climate, 20: 2133–2146.

Levitus, S., Antonov, J. I., Boyer, T. P., and Stephens, C. 2000. Warming of the world ocean. Science, 287: 2225–2229.

Llopiz, J. K., Richardson, D. E., Shiroza, A., Smith, S. L., and Cowen, R. K. 2010. Distinctions in the diets and distributions of larval tunas and the important role of appendicularians. Limnology and Oceanography, 55: 983–996.

Lutcavage, M. E., Brill, R. W., Skomal, G. B., Chase, B. C., Goldstein, J. L., and Tutein, J. 2000. Tracking adult North Atlantic bluefin tuna (*Thunnus thynnus*) in the northwestern Atlantic using ultrasonic telemetry. Marine Biology, 137: 347–358.

Lutcavage, M. E., Brill, R. W., Skomal, G. B., Chase, B. C., and Howey, P. W. 1999. Results of pop-up satellite tagging of spawning size class fish in the Gulf of Maine: do North Atlantic bluefin tuna spawn in the mid-Atlantic? Canadian Journal of Fisheries and Aquatic Sciences, 56: 173–177.

Masuma, S., Miyashita, S., Yamamoto, H., and Kumai, H. 2008. Status of bluefin tuna farming, broodstock management, breeding and fingerling production in Japan. Reviews in Fisheries Science, 16: 385–390.

Masuma, S., Tezuka, N., Koiso, M., Jinbo, T., Takebe, T., Yamazaki, H., Obana, H., *et al.* 2006. Effects of water temperature on bluefin tuna spawning biology in captivity. Bulletin of the Fisheries Research Agency of Japan, 4(Suppl.): 157–172.

McAllister, M. K., and Carruthers, T. 2008. 2007 stock assessment and projections for western Atlantic bluefin tuna using a BSP and other SRA methodology. ICCAT Collective Volume of Scientific Papers, 62: 1206–1270.

Medina, A., Abascal, F. J., Megina, C., and Garcia, A. 2002. Stereological assessment of the reproductive status of female Atlantic northern bluefin tuna during migration to Mediterranean spawning grounds through the Strait of Gibraltar. Journal of Fish Biology, 60: 230–217.

Miyashita, S., Yuji, T., Yoshifumi, S., Osamu, M., Nobuhiro, H., Kenji, T., and Toshio, M. 2000. Embryonic development and effects of water temperature on hatching of the bluefin tuna, *Thunnus thynnus*. Suisan Zoshoku, 48: 199–207.

Muhling, B. A., Lamkin, J. T., and Roffer, M. A. 2010. Predicting the occurrence of Atlantic bluefin tuna (*Thunnus thynnus*) larvae in the northern Gulf of Mexico: building a classification model from archival data. Fisheries Oceanography, 19: 526–539.

Muller-Karger, F. E., Walsh, J. J., Evans, R. H., and Meyers, M. B. 1991. On the seasonal phytoplankton concentration and sea surface temperature cycles of the Gulf of Mexico as determined by satellites. Journal of Geophysical Research, 96: 12645–12665.

Nakicenovic, N., and Swart, R. (eds). 2000. Special Report on Emissions Scenarios. Cambridge University Press, Cambridge, UK. 612 pp.

Perry, A. L., Low, P. J., Ellis, J. R., and Reynolds, J. D. 2005. Climate change and distribution shifts in marine fishes. Science, 308: 1912–1915.

Perry, R. I., Cury, P., Brander, K., Jennings, S., Möllmann, C., and Planque, B. 2010. Sensitivity of marine systems to climate and fishing: concepts, issues and management responses. Journal of Marine Systems, 79: 427–435.

Planque, B., Fromentin, J-M., Cury, P., Drinkwater, K. F., Jennings, S., Perry, R. I., and Kifani, S. 2010. How does fishing alter marine populations and ecosystems sensitivity to climate? Journal of Marine Systems, 79: 403–417.

Polovina, J. J. 2007. Decadal variation in the trans-Pacific migration of northern bluefin tuna (*Thunnus thynnus*) coherent with climate-induced change in prey abundance. Fisheries Oceanography, 5: 114–119.

Polovina, J. J., Mitchum, G. T., Graham, N. E., Craig, M. P., DeMartini, E. E., and Flint, E. N. 2007. Physical and biological consequences of a climate event in the central North Pacific. Fisheries Oceanography, 3: 15–21.

Pörtner, H. O., and Peck, M. A. 2010. Climate change impacts on fish and fisheries: towards a cause and effect understanding. Journal of Fish Biology, 77: 1745–1779.

Ravier, C., and Fromentin, J-M. 2004. Are the long-term fluctuations in Atlantic bluefin tuna (*Thunnus thynnus*) population related to environmental changes? Fisheries Oceanography, 13: 145–160.

Richards, W. J. 1976. Spawning of bluefin tuna (*Thunnus thynnus*) in the Atlantic Ocean and adjacent seas. ICCAT Collective Volume of Scientific Papers, 5: 267–278.

Richards, W. J., McGowan, M. F., Leming, T., Lamkin, J. T., and Kelley, S. 1993. Larval fish assemblages at the Loop Current boundary in the Gulf of Mexico. Bulletin of Marine Science, 53: 475–537.

Roessig, J. M., Woodley, C. M., Cech, J. J., and Hansen, L. J. 2004. Effects of global climate change on marine and estuarine fishes and fisheries. Reviews in Fish Biology and Fisheries, 14: 251–275.

Rooker, J. R., Bremer, J. R. A., Block, B. A., Dewar, H., De Metrio, G., Corriero, A., Kraus, R. T., *et al.* 2007. Life history and stock structure of Atlantic bluefin tuna (*Thunnus thynnus*). Reviews in Fisheries Science, 15: 265–310.

Scavia, D., Field, J. C., Boesch, D. F., Buddemeier, R. W., Burkett, V., Cayan, D. R., Fogarty, M., *et al.* 2002. Climate change impacts on US coastal and marine ecosystems. Estuaries, 25: 149–164.

Schaefer, K. M. 2001. Reproductive biology. *In* Tunas: Physiology, Ecology and Evolution, pp. 225–270. Ed. by B. A. Block, and E. D. Stevens. Academic Press, San Diego, CA.

Scott, G. P., Turner, S. C., Grimes, C. B., Richards, W. J., and Brothers, E. B. 1993. Indices of larval bluefin tuna, *Thunnus thynnus*, abundance in the Gulf of Mexico: modeling variability in growth, mortality, and gear selectivity: ichthyoplankton methods for estimating fish biomass. Bulletin of Marine Science, 53: 912–929.

Sherrod, P. H. 2003. DTREG: classification and regression trees for data mining and modeling. www.dtreg.com/DTREG.pdf (Accessed September 2009).

Stokesbury, M. J. W., Teo, S. L. H., Seitz, A., O'Dor, R. K., and Block, B. A. 2004. Movement of Atlantic bluefin tuna (*Thunnus thynnus*) as determined by satellite tagging experiments initiated off New England. Canadian Journal of Fisheries and Aquatic Sciences, 61: 1976–1987.

Teo, S. L. H., Boustany, A. M., and Block, B. A. 2007a. Oceanographic preferences of Atlantic bluefin tuna *Thunnus thynnus* on their Gulf of Mexico breeding grounds. Marine Biology, 152: 1105–1119.

Teo, S. L. H., Boustany, A., Dewar, H., Stokesbury, M. J. W., Weng, K. C., Beemer, S., Seitz, A. C., *et al.* 2007b. Annual migrations, diving behavior, and thermal biology of Atlantic bluefin tuna, *Thunnus thynnus*, on their Gulf of Mexico breeding grounds. Marine Biology, 151: 1–18.

Vayssieres, M. P., Plant, R. E., and Allen-Diaz, B. H. 2000. Classification trees: an alternative non-parametric approach for predicting species distributions. Journal of Vegetation Science, 11: 679–694.

Wang, C., Enfield, D. B., Lee, S-K., and Landsea, C. W. 2006. Influences of the Atlantic Warm Pool on western hemisphere summer rainfall and Atlantic hurricanes. Journal of Climate, 19: 3011–3028.

Wang, C., and Lee, S-K. 2007. Atlantic Warm Pool, Caribbean low-level jet, and their potential impact on Atlantic hurricanes. Geophysical Research Letters, 34. doi:10.1029/2006GL028579.

Wennekens, M. P. 1959. Water mass properties of the Straits of Florida and related waters. Bulletin of Marine Science, 9: 1–52.